

Guaiacol-enhanced laccase secretion by *Trametes versicolor* for lignin modification toward high-performance bamboo composites

Yingjie Wang^{a,1}, Yu Qin^{a,1}, Jieyu Yang^a, Guanben Du^a, Mizi Fan^b, Yan Xia^{a,*},
Xiaojian Zhou^a, Yonghui Zhou^c, Jingjing Liao^d

^a Yunnan Provincial Key Laboratory of Wood and Bamboo Biomass Materials, Southwest Forestry University, Kunming 650224, China

^b College of Engineering, Design and Physical Sciences, Brunel University London, Uxbridge UB8 3PH, UK

^c College of Materials and Energy, South China Agricultural University, Guangzhou 510642, China

^d Yunnan Agricultural University, Kunming 650201, China

ARTICLE INFO

Keywords:

Bamboo composites
Trametes versicolor
Laccase induction
Lignin depolymerisation
Interfacial bonding
Mechanical enhancement

ABSTRACT

This study reports high-performance bamboo-based composites engineered through a biological eco-modification strategy involving targeted lignin depolymerisation. By leveraging guaiacol-enhanced *Trametes versicolor* pretreatment, we achieved substantial improvements in the mechanical properties and water resistance of bamboo-phenolic resin composites via efficient biological modification of *Dendrocalamus sinicus*. This targeted biological modification boosted laccase activity to 2566.28 U/L, selectively depolymerised lignin and hemicellulose (by 6.97% and 11.46%, respectively) while preserving the cell wall skeleton, increased the crystallinity of bamboo from 28.28% to 31.94%, and enhanced the surface reactivity of bamboo for subsequent resin bonding. This bioconversion enhanced bamboo's chemical reactivity via targeted lignin demethoxylation and β -O-4 bond cleavage, efficiently generating additional phenolic hydroxyl groups, while also improving surface wettability (contact angle reduced from 109.73° to 79.96°) to facilitate resin penetration. Consequently, the resulting composites exhibited superior fiber-resin interfacial bonding, leading to exceptional mechanical performance, with tensile strength reaching 286.65 MPa (40.2% higher than untreated controls) and bonding strength of 9.74 MPa (33.6% improvement). Furthermore, the composites demonstrated enhanced water resistance and interfacial stability, underscoring their suitability for load-bearing applications. This targeted lignin depolymerisation strategy directly optimises the bamboo-resin interface, offering a sustainable pathway for the industrial production of high-strength biocomposites and enabling the value-added utilisation of bamboo resources.

1. Introduction

Bamboo has emerged as a promising industrial lignocellulosic feedstock for replacing traditional wood composites, in line with the demand for sustainable and low-carbon materials (Huang et al., 2024; Wang J. et al., 2022). However, the widespread application of bamboo-based composite materials is hindered by challenges such as poor interfacial compatibility between bamboo fibres and polymer matrices, as well as the high energy consumption associated with bamboo pretreatment (Lei et al., 2025; Liu et al., 2025; Xu et al., 2025). The inherently dense cellular structure and unfavourable surface chemistry of bamboo impede effective resin infiltration and bonding, significantly

compromising interfacial bonding. To address these limitations, eco-friendly biological methods such as fungal pretreatment have emerged as promising alternatives (Liu et al., 2017; M.R. et al., 2019; Xu et al., 2025). White-rot fungi, particularly *Trametes versicolor* (*T. versicolor*), are highly effective in this context due to their unique enzymatic systems.

T. versicolor is capable of selective ligninolysis, mediated primarily by its extracellular enzyme system (laccase, MnP, and LiP), which preferentially modifies and depolymerises lignin over polysaccharides under controlled cultivation conditions. Laccase depolymerises lignin in the bamboo matrix to generate highly reactive small molecules, including phenols, aldehydes, and ketones. These modifications alter the

* Correspondence to: Southwest Forestry University, Kunming 650224, China.

E-mail addresses: Mizi.Fan@brunel.ac.uk (M. Fan), xiayanswf@gmail.com (Y. Xia).

¹ These two authors contributed equally to the work.

surface chemistry and microstructure of bamboo fibres, thereby improving wettability and fibre-matrix adhesion, which are critical for enhancing the mechanical performance of the resulting composites (Enriquez-Medina et al., 2024; Fei et al., 2023; Zhou et al., 2025). Nevertheless, the efficiency of fungal pretreatment is highly dependent on strain selection, incubation conditions, and substrate composition (Zhang et al., 2023). The limited efficacy of *T. versicolor* on bamboo under standard culture conditions, as evidenced by its low ligninolytic activity and restricted delignification, was overcome by developing a guaiacol-amended culture medium. As a lignin-derived laccase inducer, guaiacol significantly enhanced enzyme production and delignification efficiency. The resulting bio-pretreatment not only improved the targeted delignification selectivity but also enhanced the interfacial compatibility of subsequent composites, which is beneficial for facilitating the scalable production of high-performance bamboo composites (Wu et al., 2024).

This study focuses on *Dendrocalamus sinicus* (*D. sinicus*), a bamboo species renowned for its rapid growth and exceptional mechanical strength. Nevertheless, its potential remains underexploited due to unfavourable interfacial properties with polymer matrices. We propose an innovative strategy that integrates guaiacol-induced fungal pretreatment with phenolic resin bonding to fabricate high-performance bamboo composites. This strategy employs guaiacol to selectively induce an efficient laccase-producing regime in *T. versicolor*, characterised by high lignin oxidative enzyme activities but suppressed cellulase activity. The resulting high selectivity favours the targeted modification and degradation of lignin over cellulose, leading to its effective lignin depolymerisation and a concurrent increase in *D. sinicus* crystallinity (Qi et al., 2022). These modifications improve fibre wettability and interfacial compatibility with the resin, leading to superior bonding and composite performance. Using a multiscale methodology, we establish critical links between molecular-level changes and macroscopic material properties, thereby elucidating the mechanism underlying the performance enhancement. This integrated bio-pretreatment and resin impregnation strategy advances the development of high-performance and sustainable bamboo composites, contributing to the global pursuit of low-carbon material solutions.

2. Materials and methods

2.1. Materials

The *D. sinicus* specimens were collected from Lincang City, Yunnan province, China. After removing the green and yellow outer layers, defect-free sections were selected for subsequent experiments. The white-rot fungus *T. versicolor* (Strain No.: CFCC5336) was provided by the China Forestry Culture Collection Centre. All the following reagents, of analytical grade and used directly without further purification, were obtained from Sinopharm Chemical Reagent Co. Ltd.: KH_2PO_4 (CAS: 7778-77-0, 99.5% purity), $\text{MgSO}_4 \cdot 7 \text{H}_2\text{O}$ (CAS: 10034-99-8, 99.0% purity), ammonium tartrate (CAS: 3164-29-2, 99.0% purity), guaiacol (CAS: 90-05-1, 99.0% purity), carboxy-methylcellulose (CAS: 9004-32-4, 98% purity), avicel (CAS: 9004-34-6, 94% purity), xylan (CAS: 9014-63-5, 90% purity), starch (CAS: 9005-25-8, 98% purity), pectin (CAS: 9000-69-5, 99% purity), 2,2'-azino-bis (3-ethylbenzothiazoline-6-sulfonic acid) (ABTS) (CAS: 30931-67-0, 98% purity), MnSO_4 (CAS: 10034-96-5, $\geq 99\%$ purity), and veratryl alcohol (CAS: 93-03-8, 98% purity). Phenol-formaldehyde (PF) resin was supplied by Zhuhai Shengquan Hi-Tech Materials Co., Ltd.

2.2. Design of guaiacol-amended culture media for laccase induction

The basal culture medium for both groups was prepared by adding a defined trace element solution, KH_2PO_4 , $\text{MgSO}_4 \cdot 7 \text{H}_2\text{O}$, and ammonium tartrate to distilled water. Then, 400 mL of the medium was dispensed into 500 mL Erlenmeyer flasks, each containing 25 bamboo strips

(70 mm (longitudinal) \times 10 mm (radial) \times 1 mm (tangential)), according to the specifications of GB/T 15780-1995, supplemented with 10 g of bamboo powder as the primary carbon source. This prepared medium served directly for the Tv-basal group. For the Tv-induced group, the medium was further supplemented with 1.0 mmol/L guaiacol on day 4 of cultivation to enhance the laccase activity of the white-rot fungus. The terms Tv-basal and Tv-induced designate the basal and guaiacol-induced *T. versicolor* pretreatment systems, respectively.

2.3. Guaiacol-induced fungal pretreatment for targeted lignin depolymerisation

Initially, *D. sinicus* was cut into strips with dimensions of 70 mm (longitudinal) \times 10 mm (radial) \times 1 mm (tangential). Twenty-five strips were placed in each flask, immersed in the aforementioned liquid culture medium, and autoclaved at 121 °C for 1 h. Following sterilisation and subsequent cooling of the flasks, each flask was aseptically inoculated with 30 pieces of *T. versicolor*-colonized agar plugs (approximately 10 mm \times 10 mm). The cultures were then incubated at 28 °C for 30 days in a rotary shaker at 180 rpm to facilitate fungal pretreatment. Throughout the pretreatment period, supernatant samples were collected every five days for enzyme activity assays.

2.4. Assay of enzymatic activities to monitor fungal metabolic specificity

2.4.1. Quantification of lignin oxidative enzyme activities

The activities of laccase, manganese peroxidase (MnP), and lignin peroxidase (LiP) were assayed using ABTS, MnSO_4 , and veratryl alcohol as substrates, respectively (Arnstadt et al., 2016). All assays were conducted in optimal pH buffers to maintain pH stability: laccase activity was measured in 0.1 M acetate buffer (pH 4.5); MnP activity was measured in 0.1 M citrate buffer (pH 4.4) containing 10 mM MnSO_4 and 10 mM H_2O_2 ; and LiP activity was measured in 0.1 M citrate buffer (pH 3.0) containing 2 mM veratryl alcohol and 10 mM H_2O_2 . These three enzyme activities were determined by UV-visible spectrophotometry by monitoring absorbance changes at 420 nm for laccase, 240 nm for MnP, and 310 nm for LiP, respectively. One unit (U) of enzyme activity was defined as the amount of enzyme required to oxidise 1 μmol of substrate per minute. For each sample, three replicates were performed, and the results are presented as mean \pm standard deviation (SD).

2.4.2. Quantification of hydrolytic enzyme activities

The activities of polysaccharide hydrolases, namely endoglucanase, exoglucanase, xylanase, amylase, and pectinase, were assayed using the 3,5-dinitrosalicylic acid (DNS) method (Elissetche et al., 2007), with sodium carboxymethyl cellulose, microcrystalline cellulose, hemicellulose, starch, and pectin employed as their respective substrates. Briefly, the crude enzyme solution was incubated with each substrate at 50 °C for 10 min. Following the incubation, the DNS reagent was added, and the mixture was heated in a boiling water bath for 5 min. The absorbance was subsequently measured at 540 nm using a UV-visible spectrophotometer.

2.5. Fabrication of bamboo composites

Three bamboo strips were aligned in parallel with PF resin applied at a spread rate of 160 g/m². The assembly was hot-pressed at 150 °C under a pressure of 5 MPa for 10 min to form the bamboo biocomposite. After hot-pressing, the composite was cooled to room temperature for further characterisation. The PF resin used possessed a viscosity of 475 mPa-s and a solid content of 52.0%, measured at 25 °C.

2.6. Multiscale characterisation of pretreated bamboo

2.6.1. Evaluation of mass loss and surface wettability

2.6.1.1. Determination of mass loss. At 10-day intervals throughout the pretreatment process, sets of bamboo strips were collected. The surface mycelium was carefully removed by rinsing with distilled water, and the samples were then oven-dried and weighed to a precision of 0.0001 g. The mass loss rate was calculated based on the difference in the absolute dry mass measured before and after treatment with *T. versicolor*.

2.6.1.2. Measurement of surface wettability. The surface wettability of the *T. versicolor*-pretreated bamboo samples was evaluated using a contact angle goniometer (JC 2000 C1, Powere, China). A 2 μ L droplet of deionised water was carefully deposited onto the sample surface using a 10 μ L microsyringe. Images of the droplet were immediately captured using an integrated camera, and the contact angle was determined via accompanying analysis software. For each sample, measurements were performed at five distinct locations, and the mean value of three replicate readings at each location was reported as the final contact angle.

2.6.2. Analysis of chemical composition and structural evolution

2.6.2.1. FTIR analysis of functional group changes. Changes in functional groups and chemical structures of bamboo following white-rot fungal pretreatment were characterised by Fourier transform infrared (FT-IR) spectra (Nicolet 6700, Thermo Fisher, USA) with 32 scans. Samples were ground into a fine powder (40–60 mesh), dried at 103 ± 2 °C for 2 h, thoroughly mixed with KBr (1:100, w/w), and subsequently pressed into transparent pellets for analysis.

2.6.2.2. XRD analysis of bamboo crystallinity. To evaluate changes in crystallinity of bamboo samples following fungal pretreatment, the samples were ground to a particle size of 60–80 mesh and analysed using an X-ray diffractometer (Rigaku Miniflex 600, Japan) operating at 40 kV and 40 mA. Scans were performed from 5° to 40° (2 θ) with a step size of 0.02° and a scanning speed of 8.0 °/min. The crystallinity index (CrI) was calculated using the peak area method. Raw XRD data were processed with MDI Jade software, including baseline subtraction and peak fitting. The CrI value was determined as the ratio of the crystalline peak area to the total area (crystalline + amorphous) after deconvolution.

2.6.2.3. Chemical composition analysis. The chemical composition of bamboo, both before and after treatment with *T. versicolor*, was determined according to the standard protocols established by the National Renewable Energy Laboratory (NREL). Acid-soluble lignin content was quantified by UV-visible spectrophotometry, while acid-insoluble lignin and total cellulose content were analysed following the Chinese National Standard GB/T 2677.10–1995.

2.6.2.4. NMR characterisation of lignin structural changes. Double enzymatic lignin (DEL) was isolated from bamboo powder both before and after fungal pretreatment via the following preparation procedure: ethanol extraction (8–10 h), drying at 103 °C (2 h), ball milling (10 h) and enzymatic hydrolysis with cellulase (50 °C, 150 rpm, 48 h). The resulting residue was thoroughly washed with hot water to remove hydrolysed carbohydrates, followed by centrifugation and freeze-drying. Structural changes in the isolated lignin were analysed using two-dimensional heteronuclear single quantum coherence (2D-HSQC) NMR spectroscopy. Approximately 20 mg of the extracted lignin was dissolved in 0.5 mL of deuterated dimethyl sulfoxide (DMSO- d_6). NMR spectra were recorded with a Bruker 500 MHz spectrometer (Bruker Scientific Instruments, USA) using the 'hsqcetgpsip3' pulse program and processed with Topspin software. The spectra were acquired with a relaxation delay of 1.5 s and 32 scans.

2.6.2.5. Analysis of phenolic hydroxyl content. A vanillin standard curve was prepared using dimethyl sulfoxide (DMSO) as the solvent. Lignin samples were dissolved in DMSO, mixed with Folin-Ciocalteu (FC) reagent and distilled water, and allowed to stand. Then, a 20% Na₂CO₃ solution was added, and the mixture was diluted to volume with water. After incubation, the absorbance of the resulting product was measured at 760 nm. The phenolic hydroxyl content was calculated based on the vanillin standard curve, with a lignin-free solution serving as the blank.

2.7. Evaluation of composite performance and interfacial properties

2.7.1. Characterisation of microstructure and resin penetration

The surface morphology and cellular pore structure of bamboo fibres during the pretreatment, along with the interfacial penetration of resin within the composites, were analysed using scanning electron microscopy (SEM; ZEISS Sigma 300, Germany) and optical microscopy (OLYMPUS IX71, Japan), respectively.

2.7.2. Testing of physical and mechanical properties

The density and water absorption of bamboo, both before and after *T. versicolor* pretreatment, were determined following the Chinese National Standard GB/T 17657–2022, with five and six replicates per group, respectively. Bonding strength and tensile strength of the bamboo composites were evaluated in accordance with GB/T 7124–2008 using a universal testing machine (DR-502 A, Dongri, China). Bonding strength was assessed using specimens with a bonded area of 10 mm \times 8.75 mm. Tensile tests were performed on both individual bamboo strips and composite specimens at a crosshead speed of 5 mm/min until failure. Six replicates were tested for each group, and mean values are reported. The sample geometries for both bonding and tensile tests are illustrated in Fig. 1.

3. Results and discussion

3.1. Specific enzymatic response driving targeted modification

During fungal pretreatment, *T. versicolor* secretes multiple enzymes, primarily lignin oxidative enzymes and glycoside hydrolases. Their activities were measured to investigate the mechanisms underlying fungal-bamboo interactions.

3.1.1. Enhanced ligninolytic activities

As illustrated in Fig. 2a, both the control and induced groups reached their peak laccase activities (1949.89 U/L and 2566.28 U/L, respectively) on day 20, substantially exceeding the previously reported highest value (1113.8 U/L)(Wang F. et al., 2023) reported for *T. versicolor* and establishing a new benchmark, which is attributed to the synergistic induction of ammonium tartrate, trace elements, and guaiacol(Huang et al., 2020). Notably, guaiacol supplementation boosted laccase activity by 31.6% compared to the Tv-basal group, primarily through upregulation of associated gene expression and signalling pathways(Zhou et al., 2025). In contrast, the activities of manganese peroxidase (MnP) and lignin peroxidase (LiP) remained low (<50 U/L), consistent with the enzymatic prioritisation of *T. versicolor*, whereby laccase dominates under standard conditions due to its multifunctionality, low metabolic cost, and stability. MnP and LiP are significantly enhanced only under specific induction conditions such as high Mn²⁺ concentrations and adequate H₂O₂ supply(Janusz et al., 2020). These results demonstrate that coordinated nutrient and inductor supplementation significantly enhances laccase production, which effectively promotes the targeted depolymerisation of lignin in the bamboo substrate. During the fungal pretreatment, laccase could drive the lignin depolymerisation via cleavage of key bonds (e.g., β -O-4, C α -C β , C α -O) and demethoxylation, subsequently generating reactive derivatives, such as reactive phenolic, aldehyde, and ketone derivatives, thereby establishing a critical mechanistic basis for the efficient

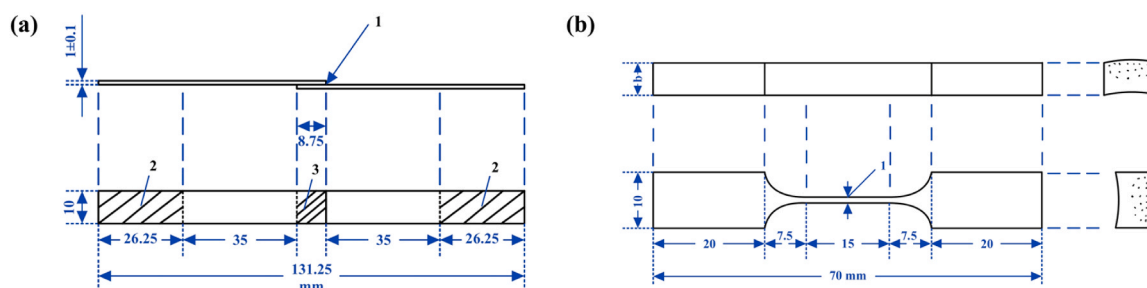


Fig. 1. Schematics of mechanical testing specimens: (a) Adhesive strength test; (b) Tensile test.

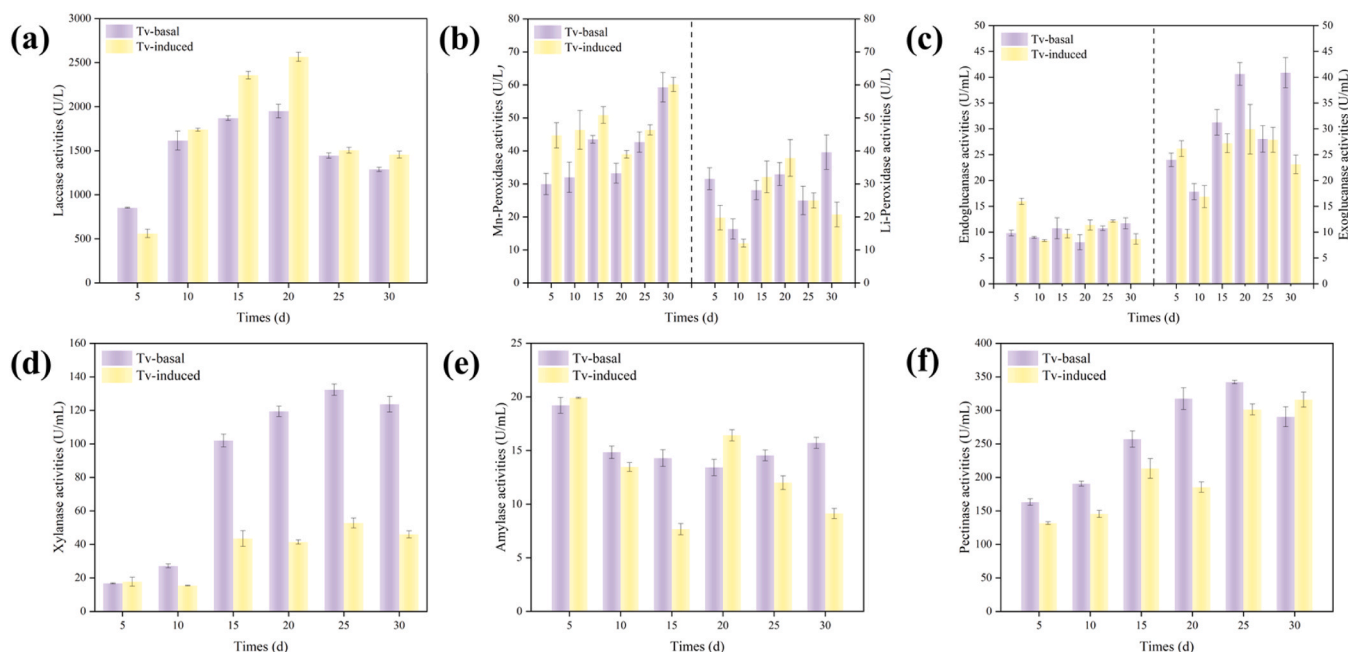


Fig. 2. Enzymatic activities of lignin oxidative enzymes and glycoside hydrolases produced by *T. versicolor* under different culture conditions: (a) Laccase; (b) Manganese peroxidase and lignin peroxidase; (c) Cellulase; (d) Xylanase; (e) Amylase; (f) pectinase.

biological modification of bamboo materials.

3.1.2. Differential regulation of hydrolytic enzyme activities

In these two experimental systems, the higher exoglucanase compared to endoglucanase activity indicated a preference for cleaving terminal cellulose bonds. Xylanase activity in both the Tv-basal and Tv-induced groups increased initially before declining. During early colonisation, pectinase activity markedly exceeded that of cellulase, xylanase, and amylase, peaking at 342.08 U/mL, which indicates that *T. versicolor* preferentially utilises pectin as a readily metabolizable carbon source (Daniel, 2016). Both Tv-basal and Tv-induced groups exhibited higher xylanase than cellulase activities. These patterns reflect that *T. versicolor* employs a prioritised enzymatic strategy that targets hemicellulose components, such as xylan, to selectively depolymerise portions of lignin and hemicellulose, thereby enabling subsequent synergistic interactions between lignin-modifying and hemicellulolytic enzymes (Sánchez, 2009). Collectively, these analyses indicate that throughout the bamboo modification process, the activity of lignin oxidative enzymes remained consistently higher and played a dominant role, whereas the activity of glycoside hydrolases was comparatively limited.

3.1.3. Evaluation of enzymatic selectivity

To quantitatively evaluate the enzymatic selectivity of the fungal pretreatment, we calculated two selectivity indices based on the

measured enzyme activities (Table 1). The lac/(cel+xyl+pec) ratio, representing the overall selectivity of ligninolytic enzymes over total polysaccharide-degrading enzymes, increased from 4.08 in the Tv-basal group to 9.99 in the Tv-induced group. More notably, the lac/cel ratio, which reflects the selectivity specifically toward cellulose preservation, increased from 47.99 to 85.77 upon guaiacol induction. These quantitative indices confirm that guaiacol not only enhances laccase activity but also selectively modulates the enzymatic profile, with a shift that prioritizes lignin degradation while largely preserving cellulose. The relatively lower lac/(cel+xyl+pec) value compared to lac/cel reflects the deliberate partial removal of pectin and hemicellulose, which is designed to optimize pore structure for subsequent resin penetration. Collectively, these data provide quantitative support for the "high selectivity" concept, with lac/cel serving as a particular indicator of cellulose preservation.

3.2. Physicochemical transformation of bamboo induced by targeted fungal pretreatment

3.2.1. Physicochemical transformation driven by selective component removal

3.2.1.1. Controlled mass loss. As shown in Fig. 3A, the most substantial mass loss in *D. sinicus* occurred within the first 10 days following treatment with *T. versicolor*. This initial phase was characterised by rapid

Table 1
Ratios of enzyme activities of Tv-basal and Tv-induced groups.

Group	lac(U/L)	cel(U/mL)	xyl(U/mL)	pec(U/mL)	lac/(cel+xyl+pec)	lac/cel
Tv-basal	1949.89	40.63	119.36	317.50	4.08	47.99
Tv-induced	2566.28	29.92	41.42	185.42	9.99	85.77

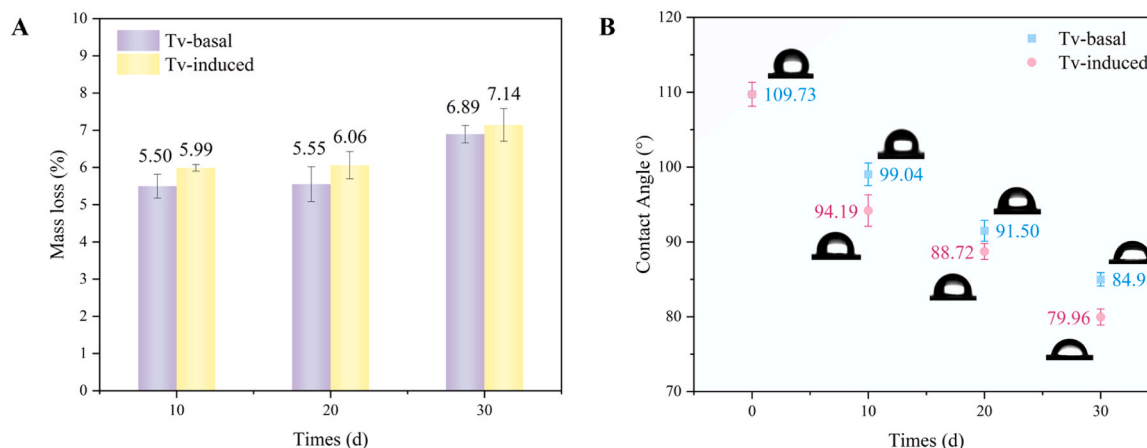


Fig. 3. Mass loss and surface wettability of *D. sinicus* during *T. versicolor* pretreatment: (A) Mass loss; (B) Contact angle before and after pretreatment.

fungal proliferation, during which hyphae colonise vascular tissues and form biofilms (Qiu et al., 2024), accompanied by the secretion of enzymes such as pectinases and hemicellulases. These enzymes act synergistically to preferentially degrade non-structural carbohydrates such as pectin (Chen et al., 2025), which serve as primary carbon sources for fungal growth. Concurrently, hemicellulose undergoes hydrolysis of glycosidic bonds in its backbone, yielding soluble oligosaccharides, such as xylo-oligosaccharides (Sohail et al., 2022), which then leach out and contribute significantly to the early-stage mass loss. Simultaneously, laccase facilitates partial depolymerisation of lignin via catalytic oxidation, thereby further contributing to mass reduction. In contrast, the Tv-basal group exhibited a minimal increase in mass loss of only 1.39 %age points between days 10 and 30, rising from 5.50% to 6.89%. Moreover, the negligible difference in mass loss between the Tv-induced and Tv-basal groups indicates that the inductor only induced a superficial activation of the bamboo substrate, which caused no significant compromise to its mechanical properties.

3.2.1.2. Improved wettability. As depicted in Fig. 3B, prolonged exposure to *T. versicolor* significantly reduced the contact angle of bamboo surfaces, indicating enhanced wettability. This change resulted from fungal-mediated modification and partial depolymerisation of lignin and hemicellulose in *D. sinicus*, which collectively enhanced the surface pore structure. By day 30, contact angles decreased to 84.98° and 79.96° for the Tv-basal and Tv-induced groups, respectively, compared to an initial value of 109.73°. This treatment by *T. versicolor* enhanced surface free energy and wettability, primarily through fungal depolymerisation of lignin via laccase and other oxidases (Elsacker et al., 2020), which disrupted the hydrophobic integrity of lignin. Concurrent hemicellulose breakdown generated hydrophilic hydroxyl groups, further improving surface hydrophilicity (Wang et al., 2018). Additionally, fungal treatment increased surface roughness, facilitating better spreading and penetration of adhesives, thereby improving the interfacial bonding in bamboo-based composites.

3.2.2. Structural and chemical evolution of the bamboo matrix

3.2.2.1. FTIR evidence of lignin modification and bond cleavage. FT-IR analysis revealed significant alterations in the chemical structure of

bamboo following pretreatment with *T. versicolor*. The attenuation of the peak at 1730 cm⁻¹, assigned to unconjugated C=O stretching in hemicellulose acetyl groups and C-O stretching in lignin ester bonds (Lian et al., 2024), indicated hemicellulose deacetylation and partial lignin depolymerisation, likely due to synergistic actions of xylanase and laccase. The gradual disappearance of the aromatic C=C vibration at 1616 cm⁻¹ (Zhao and Abu-Omar, 2016) confirmed degradation of lignin frameworks. In contrast, the peak at 1440 cm⁻¹, attributed to C-H bending in polysaccharides (Chen et al., 2017), remained stable, consistent with the low cellulase activity and the preservation of crystalline cellulose. The decreased band intensity at 1247 cm⁻¹, corresponding to phenolic ether bonds in lignin and C-O vibrations in xylan (Hormozi Jangi et al., 2020), suggests the possible occurrence of cleavage of phenolic ether bonds and partial hydrolysis of xylan, consistent with the observed increase in xylanase activity. These structural insights are in agreement with the enzymatic activity data, confirming the selective modification of bamboo by *T. versicolor*.

3.2.2.2. Microfibril realignment and increased crystallinity. Increased crystallinity of *D. sinicus* was concomitant with prolonged pretreatment time, arising from the induced chemical modifications, as determined by XRD analysis performed on whole bamboo samples rather than extracted cellulose (Fig. 4B). After 30 days, the crystallinity index (CrI) rose from 28.28% to 31.64% in the Tv-basal group and to 31.94% in the Tv-induced group. The increased intensity of cellulose diffraction peaks, without any peak shifting, indicated that fungal enzymes preferentially degraded the amorphous components (i.e., lignin and hemicellulose), thereby elevating the relative cellulose content and improving crystallite alignment (Lin et al., 2018; Wang Y.-Y. et al., 2022), while the crystalline cellulose structure remained unchanged, as evidenced by the absence of new diffraction peaks and the persistence of profiles characteristic of native cellulose (Wang Y. et al., 2023). The slightly higher CrI observed in the Tv-induced group indicates that guaiacol facilitated the removal of amorphous matrix components, thereby promoting structural ordering. Overall, the pretreatment preferentially degraded lignin and hemicellulose, thereby increasing the relative crystallinity of cellulose selectively.

3.2.2.3. Selective reduction of lignin and hemicellulose content. Chemical

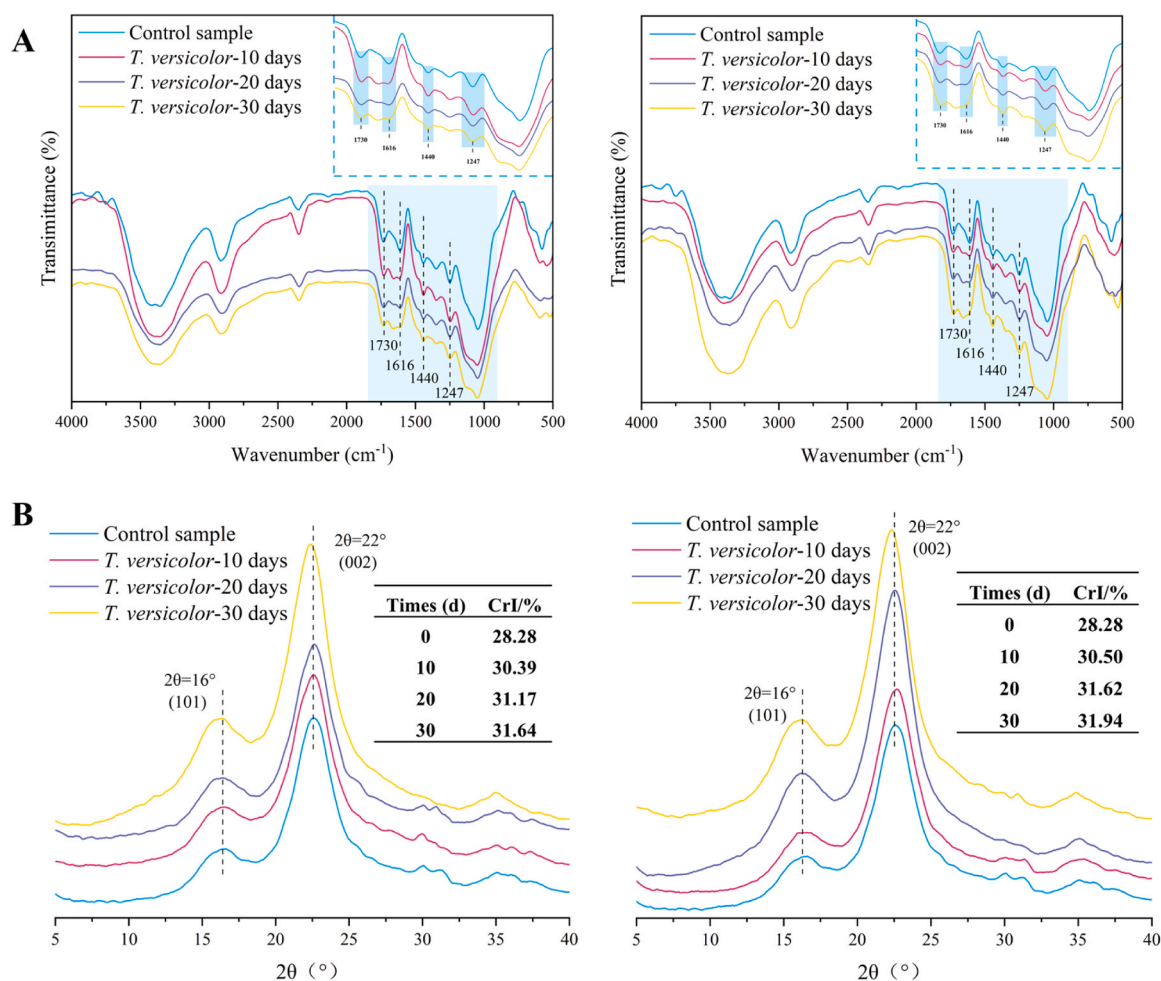


Fig. 4. Chemical and crystalline structural changes in *D. sinicus* after *T. versicolor* pretreatment: (A) FTIR spectra of Tv-basal (left) and Tv-induced (right) groups; (B) X-ray diffraction patterns and crystallinity indices of Tv-basal (left) and Tv-induced (right) groups.

composition analysis of *D. sinicus* demonstrated a time-dependent reduction in hemicellulose and lignin content following *T. versicolor* pretreatment (Table 2). After 30 days, hemicellulose and lignin contents decreased to 15.48% and 22.61% in the Tv-basal group, and to 15.07% and 22.03% in the Tv-induced group, respectively, while cellulose content significantly increased to 53.72% and 54.62%. This pattern indicates a preferential fungal degradation of lignin phenolic ether bonds and hemicellulose polysaccharide chains, disrupting their cross-linked matrix and exposing cellulose microfibrils (Bardi et al., 2017; Xu et al., 2013). The more substantial reduction in lignin content observed in the Tv-induced group is attributed to guaiacol-induced secretion of highly active laccase by *T. versicolor*, which efficiently modifies and partially depolymerises lignin in *D. sinicus*.

Table 2

Changes in chemical composition of *D. sinicus* after fungal and enzymatic pretreatment.

Group	Times (d)	Cellulose (%)	Hemicellulose (%)	Lignin (%)
Control	0	39.89	26.53	29.00
Tv-basal	10	44.62	23.02	25.59
	20	49.89	18.71	23.84
	30	53.72	15.48	22.61
Tv-induced	10	45.44	22.64	25.23
	20	50.83	18.52	23.14
	30	54.62	15.07	22.03

3.2.2.4. β -O-4 bond cleavage and lignin depolymerisation characterised by NMR. To investigate the structural changes in *D. sinicus* lignin modified by *T. versicolor*, lignin was extracted from both control and laccase-induced samples, followed by two-dimensional heteronuclear single quantum coherence (2D-HSQC) NMR analysis. Quantitative data (Table 3) and spectral assignments (Fig. 5) revealed a reduction in the methoxy (MeO) signal (δ_C/δ_H 56.0/3.70), indicating demethoxylation of lignin during fungal treatment. In the side-chain region (δ_C/δ_H 2.5–5.7/48.0–92.0) (Wen et al., 2013), key linkages, including β -O-4 aryl ether bonds (A_α , $A_\beta(G)$, $A_\beta(S)$, A'_γ) and condensed structures (β - β resinol B_ω ; β -5 phenylcoumaran C_α), were cleaved or diminished, suggesting preferential fungal attack on side-chain motifs. Quantitative analysis further showed near-complete degradation of β - β and β -5 linkages. Although

Table 3

Quantitative analysis of lignin structural units by 2D-HSQC NMR spectroscopy.

	Control sample	Tv-basal group	Tv-induced group
A(β -O-4)	48.41 ^b (89.98) ^c	56.53 ^b (100) ^c	71.42 ^b (100) ^c
B(β - β)	1.81 ^b (3.34) ^c	N.D.	N.D.
C(β -5)	3.62 ^b (6.67) ^c	N.D.	N.D.
T	3.84	3.67	1.09
FA	0.91	7.22	8.38
PCE	16.31	24.26	17.90
S	42.34	41.26	40.03
G	48.78	46.78	47.44
H	8.88	11.97	12.52

Note: N.D. not detected

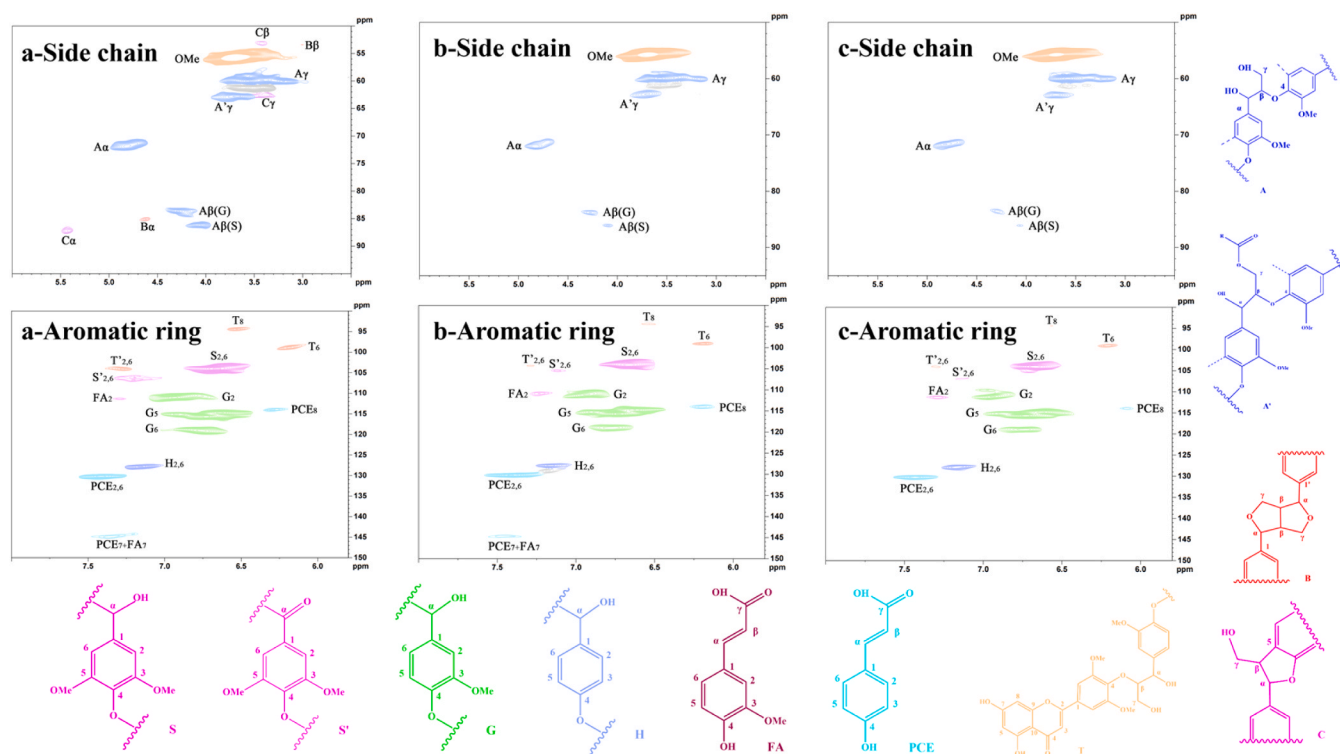


Fig. 5. 2D-HSQC NMR spectra of the side-chain and aromatic regions of *D. sinicus* lignin and its main substructures: (a) Untreated sample; (b) Tv-basal; (c) Tv-induced.

partial cleavage of β -O-4 bonds occurred, their relative abundance increased due to the extensive degradation of other lignin structural units.

In the aromatic region (δ_C/δ_H 5.7–8.0/100.0–135.0)(Wen et al., 2013), signals corresponding to syringyl (S) ($C_{2,6}$ -H_{2,6}, δ_C/δ_H 104.3/6.68), guaiacyl (G) ($C_{2,6}$ -H_{2,6}, δ_C/δ_H 113.4/6.95), and p-hydroxyphenyl (H) ($C_{2,6}$ -H_{2,6}, δ_C/δ_H 128.1/7.16) units were identified, confirming a typical grass lignin composition(Shi et al., 2013). After treatment, the signals of S and G units decreased, while the relative signal intensity of H units increased, indicating a demethoxylation-driven conversion. Notably, ferulic acid (FA) was demethoxylated to p-coumaric acid (PCE), leading to an increase in PCE, whereas triclin (T) content decreased due to demethoxylation processes. In summary, based on 2D NMR analysis and the subsequent determination of phenolic hydroxyl content by the Folin-Ciocalteu method, the laccase-mediated modification predominantly involved demethoxylation and side-chain cleavage rather than aromatic ring degradation. The observed preservation of aromatic regions alongside side-chain cleavage in lignin is consistent with the mechanism of laccase-mediated modification(Chen et al., 2021), which selectively cleaves β -O-4 linkages, generating new phenolic hydroxyl groups and enhancing lignin reactivity. The generation of new phenolic hydroxyl groups creates abundant active sites, which could form more extensive covalent cross-links with the phenolic resin adhesive during hot pressing, significantly enhancing interfacial bonding and ultimately strengthening the composite material(Yang et al., 2023).

3.2.2.5. Enhanced chemical reactivity indicated by phenolic hydroxyl content. As evident from Table 4, the phenolic hydroxyl group content in *D. sinicus* lignin increased significantly from 1.03 mmol/g in unmodified samples to 2.14 mmol/g and 2.39 mmol/g following Tv-basal and Tv-induced *T. versicolor* treatment, respectively. The higher phenolic hydroxyl content observed in the Tv-induced group signifies superior reactivity, primarily due to laccase-induced modification and partial depolymerisation of lignin. This process involves demethoxylation, side-

Table 4

Variation in phenolic hydroxyl group content in lignin of *D. sinicus* after fungal modification by *T. versicolor*.

Group	Times (d)	OH (mmol/g)
Control	0	1.03 ± 0.02
	10	1.07 ± 0.04
	20	1.59 ± 0.02
Tv-induced	30	2.14 ± 0.01
	10	1.19 ± 0.03
	20	1.79 ± 0.03
	30	2.39 ± 0.03

chain cleavage, and the generation of new phenolic hydroxyl groups, thereby increasing the number of reactive sites and enhancing overall reactivity(Jiang et al., 2019). The elevated phenolic hydroxyl groups, particularly in H-type (p-hydroxyphenyl) units, function as key reactive sites for covalent cross-linking with the phenolic resin matrix during curing(Zhao et al., 2024). Mechanistically, these phenolic hydroxyl groups undergo condensation reactions with the hydroxymethyl groups (-CH₂OH) present in the phenolic resin prepolymer(Liu et al., 2024). Under alkaline curing conditions, the nucleophilic phenolic hydroxyl attacks the electrophilic carbon of the hydroxymethyl group, leading to the formation of methylene bridges (-CH₂-) or ether linkages (-CH₂-O-CH₂-) between lignin and the resin network (Yelle and Ralph, 2016). This covalent bonding effectively integrates lignin into the three-dimensional polymer matrix, creating a robust interphase that enhances stress transfer and improves interfacial adhesion(Li et al., 2017). In summary, the increased phenolic hydroxyl content in lignin enhances its reactivity, facilitating polycondensation with the phenolic resin adhesive, enhancing bamboo surface activity, and ultimately strengthening the interfacial bonding of the bamboo-based composite.

3.3. Enhanced interfacial structure and resultant composite performance

3.3.1. Enhanced resin penetration and interfacial bonding

As shown in Fig. 6A, *T. versicolor* pretreatment formed time-dependent pores in bamboo via partial component depolymerisation, enhancing resin permeability and hot-pressing densification (Han et al., 2024). The resulting rougher, more porous surface improved interfacial bonding through deeper adhesive penetration.

Fig. 6B illustrates the adhesive infiltration within the adhesive interface of bamboo composites. Pretreatment with *T. versicolor* modified the bamboo cell wall pore structure and increased surface roughness via partial depolymerisation, enhancing resin penetration. This contrasts with the thin adhesive layer in untreated controls, which resulted from poor pore structure and poor wettability. Consequently, this resulted in a thicker adhesive interphase, as the modified pore structure provided more penetration pathways and improved wettability, promoting deeper resin infiltration and better interface bonding. With extended pretreatment duration, the thickness of the adhesive layer progressively increased, reaching 107.08 μm (Tv-basal) and 121.24 μm (Tv-induced) after 30 days, compared to 61.95 μm for the untreated control. The Tv-induced group showed greater thickness, confirming that guaiacol induction enhances fungal modification efficiency. These structural and chemical improvements facilitated deeper and more

uniform resin distribution, thereby strengthening interfacial bonding and improving the mechanical performance of the composites (Hu et al., 2023).

3.3.2. Toward high-performance biocomposites: Superior properties from tailored modification

3.3.2.1. Increased composite density. As shown in Fig. 7A, fungal pretreatment reduced bamboo density by degrading low-molecular-weight nutrients (Daniel, 2016), while composite density peaked at day 20, increasing by 8.3% in the Tv-basal group and 10.7% in the Tv-induced group. This improvement was attributed to enhanced surface wettability, modified lignin/hemicellulose reactivity, and improved resin penetration and interfacial bonding. The slight density decline by day 30 may correspond to an altered pore structure of the cell wall, suggesting that both chemical modification and resin filling contribute to the overall density increase during the optimal treatment period.

3.3.2.2. Improved water resistance. As shown in Fig. 7B, water absorption of bamboo strips and bamboo-based composites exhibited opposing trends with extended pretreatment time. Bamboo strips showed markedly increased water uptake, with the Tv-induced group reaching approximately twice that of the control after 30 days. This increase is

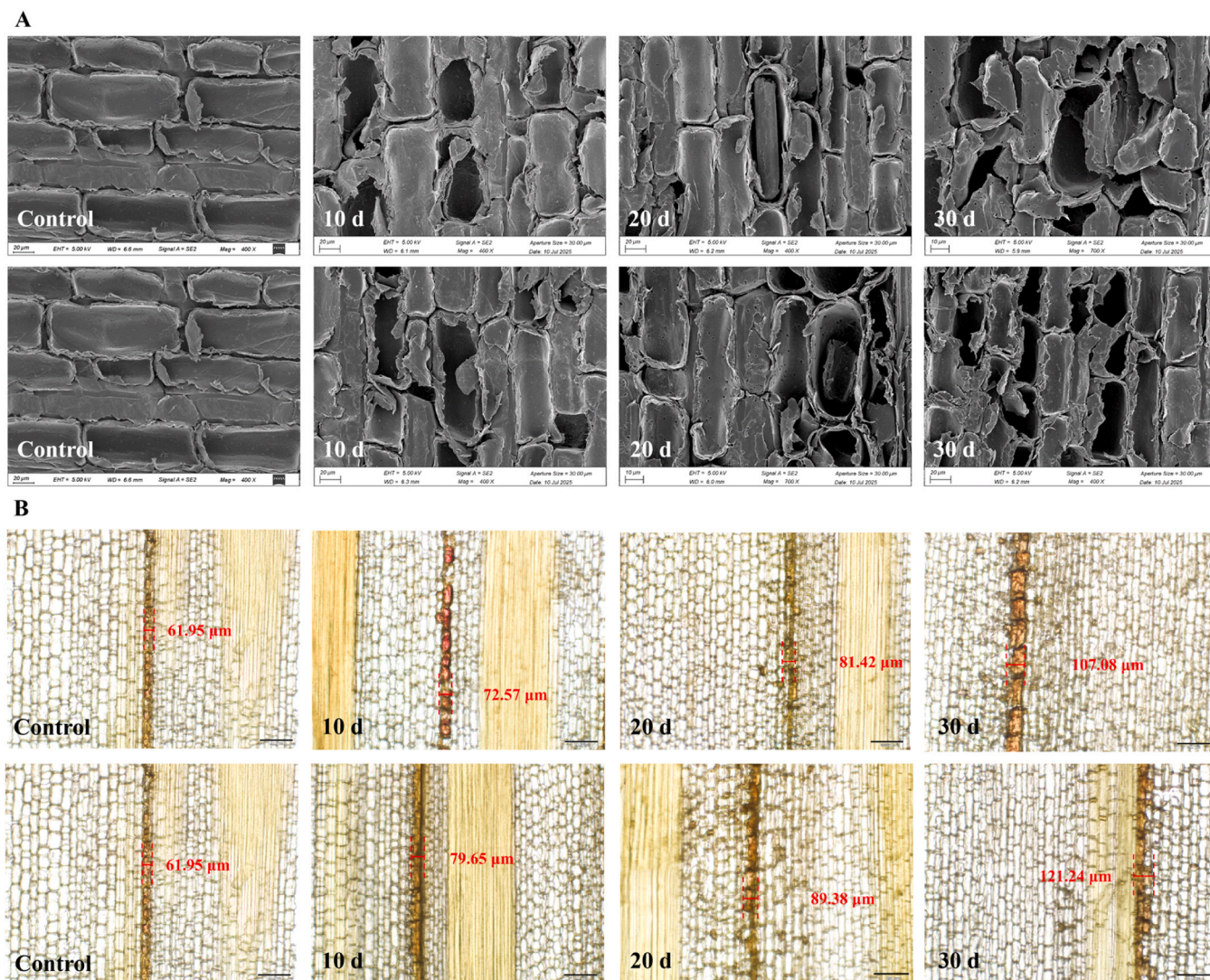


Fig. 6. Microstructure of bamboo and bamboo composites: (A) SEM images of bamboo samples from Tv-basal group (top) and Tv-induced group (bottom); (B) Adhesive interface observation of bamboo composites from Tv-basal group (top) and Tv-induced group (bottom).

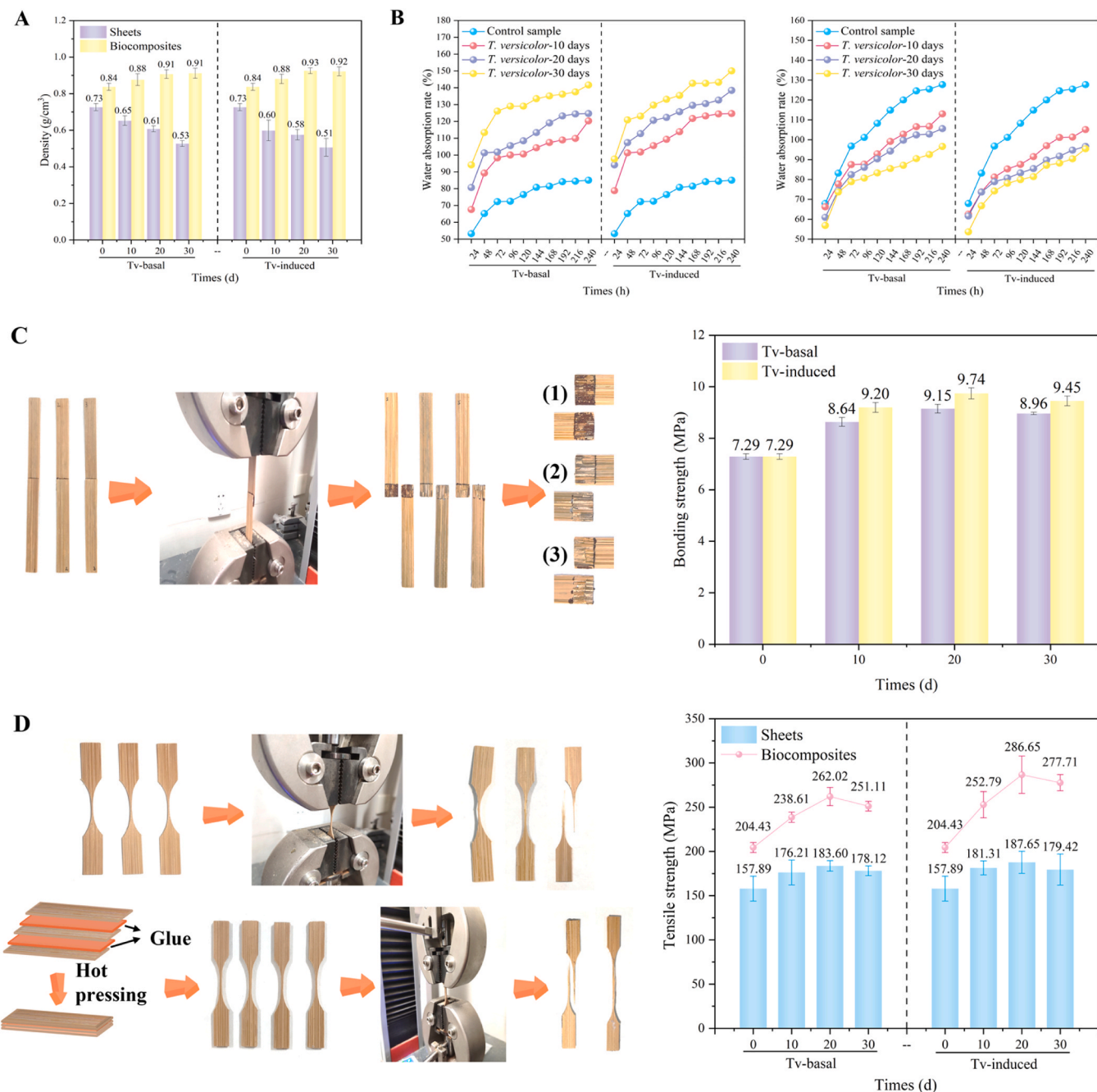


Fig. 7. Physical and mechanical characterisation of bamboo and bamboo-based composites: (A) Density; (B) Water uptake of bamboo sheets (left) and composites (right); (C) Adhesive properties: Failure modes (1–3) (left) and interfacial bond strength (right); (D) Tensile properties: Fracture behaviour (left) and tensile strength (right).

attributed to the enzymatic depolymerisation of pectin, lignin, and hemicellulose, which collectively modified the pore structure and exposed hydrophilic groups. In contrast, the composites from the Tv-basal and Tv-induced groups exhibited reductions in water absorption of 31.09% and 32.26%, respectively, compared to the control at 30 days. This improvement is attributable to effective pore-filling by phenolic resin during immersion and curing, which formed a water-resistant interphase (Yu et al., 2015). The increased composite density further inhibited water penetration through fibre compaction and covalent bonding between resin and hydroxyl groups (Abdul Khalil et al., 2008). This opposing trend reveals a dual role of fungal modification: enhancing the hydrophilicity of native bamboo while simultaneously impeding water penetration and diffusion at the interface through

improved interfacial bonding, thereby imparting hydrophobicity to the composite material. These observations indicate that the improved water resistance arises from the synergistic effect of resin filling (physical contribution) and enhanced interfacial chemical bonding (chemical contribution), rather than being dominated by a single mechanism.

3.3.2.3. Superior interfacial bonding strength achieved through optimised interface. Pretreatment with *T. versicolor* caused pronounced structural disruption in bamboo during bonding strength tests, particularly under guaiacol induction, as shown by the fracture morphology in Fig. 7C. This physical degradation was correlated with enhanced interfacial bonding: the bonding strength initially increased with prolonged pretreatment time, reaching 9.15 MPa (Tv-basal) and 9.74 MPa (Tv-induced) at 20

days, compared to 7.29 MPa in untreated bamboo. During the initial modification phase, the bonding strength of bamboo-based composites increased, primarily because the *T. versicolor* pretreatment enhanced the reactivity of lignin and hemicellulose and improved the penetration of the phenol-formaldehyde resin into bamboo cell wall, thereby suggesting the possible formation of covalent interactions and facilitating resin penetration for interface densification, which together resulted in superior interfacial bonding and enhanced mechanical properties (Chen et al., 2020; Zou et al., 2022). The Tv-induced group consistently exhibited higher strength, attributable to the stimulation of highly active laccase secretion by guaiacol induction, enabling more efficient lignin modification. However, beyond 20 days of modification, the bonding strength began to decline, likely as a result of severe structural degradation of the bamboo cell walls caused by prolonged biological pretreatment, which compromised the mechanical properties of the substrate.

3.3.2.4. Exceptional tensile strength delivered by enhanced fibre-matrix synergy. Fig. 7D (a) compares the tensile fracture behaviour between bamboo strips and bamboo-based composites. Bamboo strips exhibited a typical brittle fracture with localised breaks along weak interfaces (e.g., parenchyma cells and fibre bundle junctions), resulting from structural anisotropy that limited stress transfer. In contrast, the composites exhibited complex failure modes including fibre pull-out, bridging, and delamination (Zheng et al., 2023), resulting from multi-scale resin-fibre bonding that effectively impeded crack propagation. As summarised in Fig. 7D (b), the tensile strength of both bamboo strips and composites increased with pretreatment time, reaching maxima at 20 days. The bamboo strips attained peak strengths of 183.60 MPa (Tv-basal) and 187.65 MPa (Tv-induced), while the composites reached 262.02 MPa and 286.65 MPa, markedly higher than untreated controls (157.89 MPa and 204.43 MPa, respectively). The enzymatic action of *T. versicolor* modified and partially depolymerised lignin and hemicellulose, thereby creating a more accessible pore structure in bamboo for improved resin permeability, enhancing surface wettability for better resin spreading, and elevating lignin reactivity. These changes promoted additional condensation reactions between lignin and the phenol-formaldehyde resin and cross-linking between phenolic hydroxyl groups (from lignin) and aldehyde groups (from hemicellulose) (Yang et al., 2019), which significantly improved interfacial bonding and facilitated interfacial densification during hot pressing. The resultant composites exhibited superior tensile performance, substantially exceeding conventional bamboo laminates (89–205 MPa) and NaOH-treated bamboo (177–213 MPa). These results collectively affirm that *T. versicolor* pretreatment effectively enhances interfacial bonding and matrix reinforcement, enabling the fabrication of high-performance bamboo composites with exceptional fracture resistance and mechanical properties.

3.4. The existing strategies for lignin modification and interface design

To delineate the innovation boundary of the "guaiacol-induced laccase" strategy, this study conducted a systematic multi-dimensional comparison with common induction strategies, chemical modification methods, and traditional interface design routes (Table 5). The comparative analysis demonstrates that the guaiacol-induced strategy offers significant advantages in terms of mild reaction conditions, environmental friendliness, and excellent composite performance. Although the relatively long treatment period (20 days) is an inherent limitation of biological approaches, its low energy consumption, cost-effectiveness, and scalability render it promising for green manufacturing and sustainable development. This study provides a feasible and environmentally friendly approach for the preparation of high-performance composites via biologically modified lignin.

Table 5

Comparison of guaiacol-enhanced laccase strategy with existing approaches.

Method Category & Representative Methods	Reaction Conditions & Time	Performance Improvement	Cost, Energy Consumption & Environmental Impact
Traditional Interface Design Routes (Surface/interface optimisation: coupling agent (Peng et al., 2024), oxidation (Ding et al., 2024))	Moderate conditions; short treatment time	Enhanced interfacial bonding strength	Moderate cost; moderate energy consumption and chemical usage
Chemical Modification Methods (Direct lignin structural modification: demethylation (Li et al., 2017), hydroxymethylation (Yelle and Ralph, 2016), phenolation (Liu et al., 2024))	Harsh (100–220 °C, high pressure); short reaction time (hours) but multi-step	20–40% improvement in mechanical properties; reduced formaldehyde emission	High reagent cost and energy consumption; potential environmental pollution
Common Induction Strategies (e.g., copper ion, veratryl alcohol, xylydine) (Santana et al., 2018)	Mild (28–30 °C, atmospheric pressure); 9–24 days to peak activity	Only increases enzyme activity, no direct composite improvement	Low to medium cost; low energy consumption, and environmentally friendly
Current Study: Guaiacol-enhanced laccase secretion strategy (Efficient pretreatment with targeted enzymatic bioconversion)	Mild (28 °C, atmospheric pressure, peak laccase activity of 2566.28 U/L on day 20)	40.2% increase in tensile strength, 33.6% improvement in bonding strength, and 32.26% reduction in water absorption	Low cost and energy consumption; environmentally friendly (no toxic by-products)

4. Conclusions

This study established guaiacol-induced fungal pretreatment as an effective biological strategy for fundamentally improving the interfacial compatibility and mechanical properties of bamboo-phenolic resin composites. Guaiacol functioned as a laccase-specific inducer, upregulating lignin-degrading enzyme activity and enabling selective delignification while largely preserving cellulose and facilitating limited hemicellulose removal to enhance resin penetration. This targeted modification altered the surface pore structure of bamboo, enhanced its surface reactivity, and significantly improved wettability, thereby promoting the penetration of phenolic resin into the bamboo cell wall and strengthening the interfacial bonding in the composites. The optimised composites exhibited a 40.2% increase in tensile strength and a 33.6% improvement in bonding strength, along with a remarkable 32.26% reduction in water absorption owing to microstructural densification. These findings highlighted the critical need for precision in fungal pretreatment balancing surface activation and structural integrity. This work established a foundation for sustainable manufacturing of high-performance lignocellulosic composites, with significant property enhancements indicating strong potential for practical applications, including structural panels, automotive interiors, and construction formwork.

CRedit authorship contribution statement

Yonghui Zhou: Writing – review & editing. **Jingjing Liao:** Writing – review & editing. **Guanben Du:** Conceptualization. **Mizi Fan:** Methodology. **Yan Xia:** Supervision, Funding acquisition. **Xiaojian Zhou:**

Methodology. **Yingjie Wang:** Writing – original draft, Conceptualization. **Yu Qin:** Formal analysis. **Jieyu Yang:** Formal analysis.

Declaration of Competing Interest

The authors declare that they have no known competing financial interests or personal relationships that could have appeared to influence the work reported in this paper.

Acknowledgements

The authors are grateful for the financial support from the Regional Project of the National Natural Science Foundation of China (32260362), the Joint Project of Yunnan Agricultural Basic Research (202401BD070001–025), the Foreign Experts Project of Yunnan Province (202505AO120007), the Reserve Talent Project for Young and Middle-aged Academic and Technical Leaders of Yunnan Province (202405AC350033), and the 111 Project (D21027).

Data availability

Data will be made available on request.

References

- Abdul Khalil, H.P.S., Nur Firdaus, M.Y., Anis, M., Ridzuan, R., 2008. The effect of storage time and humidity on mechanical and physical properties of medium density fiberboard (MDF) from oil palm empty fruit bunch and rubberwood. *Polym. Plast. Technol. Eng.* 47, 1046–1053. <https://doi.org/10.1080/03602550802356644>.
- Arnstadt, T., Hoppe, B., Kahl, T., Kellner, H., Krüger, D., Bässler, C., Bauhus, J., Hofrichter, M., 2016. Patterns of laccase and peroxidases in coarse woody debris of *Fagus sylvatica*, *Picea abies* and *Pinus sylvestris* and their relation to different wood parameters. *Eur. J. For. Res* 135, 109–124. <https://doi.org/10.1007/s10342-015-0920-0>.
- Bardi, A., Yuan, Q., Siracusa, G., Chicca, I., Islam, M., Spennati, F., Tigrini, V., Di Gregorio, S., Levin, D.B., Petroni, G., Munz, G., 2017. Effect of cellulose as co-substrate on old landfill leachate treatment using white-rot fungi. *Bioresour. Technol.* 241, 1067–1076. <https://doi.org/10.1016/j.biortech.2017.06.046>.
- Chen, C., Li, Z., Mi, R., Dai, J., Xie, H., Pei, Y., Li, J., Qiao, H., Tang, H., Yang, B., Hu, L., 2020. Rapid Processing of Whole Bamboo with Exposed, Aligned Nanofibrils toward a High-Performance Structural Material. *ACS Nano* 14, 5194–5202. <https://doi.org/10.1021/acsnano.9b08747>.
- Chen, H., Yu, Y., Zhong, T., Wu, Y., Li, Y., Wu, Z., Fei, B., 2017. Effect of alkali treatment on microstructure and mechanical properties of individual bamboo fibers. *Cellulose* 24, 333–347. <https://doi.org/10.1007/s10570-016-1116-6>.
- Chen, X., Ouyang, X., Li, J., Zhao, Y.-L., 2021. Natural Syringyl Mediators Accelerate Laccase-Catalyzed β -O-4 Cleavage and Co-Oxidation of a Guaiacyl Model Substrate via an Aggregation Mechanism. *ACS Omega* 6, 22578–22588. <https://doi.org/10.1021/acsomega.1c02501>.
- Chen, Y., Tang, M., Song, Y.-C., Zargar, M., Chen, M.-X., Lin, S.-Y., Zhu, F.-Y., Song, T., 2025. Unlocking bamboo's fast growth: Exploring the vital role of non-structural carbohydrates (NSCs). *Plant J.* 122, e70147. <https://doi.org/10.1111/tpj.70147>.
- Daniel, G., 2016. Chapter 8 - Fungal Degradation of Wood Cell Walls. In: Kim, Y.S., Funada, R., Singh, A.P. (Eds.), *Secondary Xylem Biology*. Academic Press, Boston, pp. 131–167. <https://doi.org/10.1016/B978-0-12-802185-9.00008-5>.
- Ding, R., Liu, X., Yu, H., Shi, S.Q., Han, G., Cheng, W., 2024. Effects of different oxidation systems on the interfacial properties of bamboo fiber/epoxy resin composites. *Surf. Interfaces* 45, 103843. <https://doi.org/10.1016/j.surfin.2024.103843>.
- Elissetche, J.-P., Ferraz, A., Freer, J., Rodríguez, J., 2007. Enzymes produced by *Ganoderma australe* growing on wood and in submerged cultures. *World J. Microbiol. Biotechnol.* 23, 429–434. <https://doi.org/10.1007/s11274-006-9243-0>.
- Elsacker, E., Vandeloek, S., Van Wylick, A., Ruytinx, J., De Laet, L., Peeters, E., 2020. A comprehensive framework for the production of mycelium-based lignocellulosic composites. *Sci. Total Environ.* 725, 138431. <https://doi.org/10.1016/j.scitotenv.2020.138431>.
- Enriquez-Medina, I., Rodas-Ortiz, I., Bedoya-García, I., Velasquez-Godoy, A., Alvarez-Vasco, C., Ceballos Bermudez, A., 2024. Bridging gap between agro-industrial waste, biodiversity and mycelium-based biocomposites: Understanding their properties by multiscale methodology. *J. Bioresour. Bioprod.* 9, 495–507. <https://doi.org/10.1016/j.jobab.2024.07.001>.
- Fei, B., Wang, D., AlMasoud, N., Yang, H., Yang, J., Alomar, T.S., Puangsin, B., Xu, B.B., Algadi, H., El-Bahy, Z.M., Guo, Z., Shi, Z., 2023. Bamboo fiber strengthened poly (lactic acid) composites with enhanced interfacial compatibility through a multi-layered coating of synergistic treatment strategy. *Int. J. Biol. Macromol.* 249, 126018. <https://doi.org/10.1016/j.ijbiomac.2023.126018>.
- Han, S., Zhao, Xiang, Li, Xinpu, Ye, Hanzhou, Wang, G., 2024. Synergistic in-situ reinforcement of lignin and adhesive for high-performance aligned bamboo fibers composites. *J. Mater. Res. Technol.* 28, 879–890. <https://doi.org/10.1016/j.jmrt.2023.12.042>.
- Hormozi Jangi, S.R., Akhond, M., Dehghani, Z., 2020. High throughput covalent immobilization process for improvement of shelf-life, operational cycles, relative activity in organic media and enzymatic kinetics of urease and its application for urea removal from water samples. *Process Biochem.* 90, 102–112. <https://doi.org/10.1016/j.procbio.2019.11.001>.
- Hu, J., Wu, J., Huang, Y., He, Y., Lin, J., Zhang, Yamei, Zhang, Yahui, Yu, Y., Yu, W., 2023. Super-strong biomimetic bulk bamboo-based composites by a neural network interfacial design strategy. *Chem. Eng. J.* 475, 146435. <https://doi.org/10.1016/j.cej.2023.146435>.
- Huang, S., Huang, D., Wu, Q., Hou, M., Tang, X., Zhou, J., 2020. Effect of environmental C/N ratio on activities of lignin-degrading enzymes produced by *Phanerochaete chrysosporium*. *Pedosphere* 30, 285–292. [https://doi.org/10.1016/S1002-0160\(17\)60391-6](https://doi.org/10.1016/S1002-0160(17)60391-6).
- Huang, X., Chen, X., Xian, Y., Jiang, F., 2024. The material sources, pharmacological activities of bamboo polysaccharides and influencing factors: a review. *Ind. Crops Prod.* 210, 118037. <https://doi.org/10.1016/j.indcrop.2024.118037>.
- Janusz, G., Pawlik, A., Świdarska-Burek, U., Polak, J., Sulej, J., Jarosz-Wilkolazka, A., Paszczyński, A., 2020. Laccase properties, physiological functions, and evolution. *Int. J. Mol. Sci.* 21, 966. <https://doi.org/10.3390/ijms21030966>.
- Jiang, L., Guo, H., Li, C., Zhou, P., Zhang, Z., 2019. Selective cleavage of lignin and lignin model compounds without external hydrogen, catalyzed by heterogeneous nickel catalysts. *Chem. Sci.* 10, 4458–4468. <https://doi.org/10.1039/C9SC00691E>.
- Lei, W., Wang, S., Xia, Y., Yang, Y., Zhang, Y., Yu, W., 2025. Novel strategy for preparing high-performance bamboo-fiber-reinforced composite by designing bonding interface. *Ind. Crops Prod.* 233, 121388. <https://doi.org/10.1016/j.indcrop.2025.121388>.
- Li, Jiongjiang, Zhang, J., Zhang, S., Gao, Q., Li, Jianzhang, Zhang, W., 2017. Fast curing bio-based phenolic resins via lignin demethylated under mild reaction condition. *Polymers* 9, 428. <https://doi.org/10.3390/polym9090428>.
- Lian, H., Li, P., Xu, Y., Zhang, X., 2024. A simple and sustainable method for preparing high-strength, lightweight, dimensional stable, and mildew resistant multifunctional bamboo. *Constr. Build. Mater.* 415, 135027. <https://doi.org/10.1016/j.conbuildmat.2024.135027>.
- Lin, J., Yang, Z., Hu, X., Hong, G., Zhang, S., Song, W., 2018. The effect of alkali treatment on properties of dopamine modification of bamboo fiber/poly(lactic acid) composites. *Polymers* 10, 403. <https://doi.org/10.3390/polym10040403>.
- Liu, J., Zhu, Y., Gong, Z., Chang, Z., Meng, Y., Qu, W., Zhao, C., Li, M., Zhu, C., 2024. Preparation and characterization of lignin copolymerized phenolic resins with superior stiffening effect for natural rubber composites. *Polymer* 308, 127366. <https://doi.org/10.1016/j.polymer.2024.127366>.
- Liu, M., Baum, A., Odermatt, J., Berger, J., Yu, L., Zeuner, B., Thygesen, A., Holck, J., Meyer, A.S., 2017. Oxidation of lignin in hemp fibres by laccase: Effects on mechanical properties of hemp fibres and unidirectional fibre/epoxy composites. *Compos. Part A Appl. Sci. Manuf.* 95, 377–387. <https://doi.org/10.1016/j.compositesa.2017.01.026>.
- Liu, W., Yang, F., Qing, L., Gao, S., Zhang, A., 2025. High-strength bamboo fiber (HSBF) and bamboo fiber reinforced epoxy composites (BFRECs): preparation, tensile performance and water-proof effect of resin precoat (RPC) treatment. *Ind. Crops Prod.* 236, 121844. <https://doi.org/10.1016/j.indcrop.2025.121844>.
- M.R. S., Siengchin, S., Parameswaranpillai, J., Jawaid, M., Pruncu, C.I., Khan, A., 2019. A comprehensive review of techniques for natural fibers as reinforcement in composites: preparation, processing and characterization. *Carbohydr. Polym.* 207, 108–121. <https://doi.org/10.1016/j.carbpol.2018.11.083>.
- Peng, Z., Yu, M., Niu, Y., Du, X., Gao, S., 2024. Enhanced mechanical, thermal, water and UV aging resistance properties of bamboo fiber/HDPE composites through silane coupling agent modified nano-SiO₂-TiO₂. *Ind. Crops Prod.* 222, 119704. <https://doi.org/10.1016/j.indcrop.2024.119704>.
- Qi, J., Jia, L., Liang, Y., Luo, B., Zhao, R., Zhang, C., Wen, J., Zhou, Y., Fan, M., Xia, Y., 2022. Fungi's selectivity in the biodegradation of *Dendrocalamus sinicus* decayed by white and brown rot fungi. *Ind. Crops Prod.* 188, 115726. <https://doi.org/10.1016/j.indcrop.2022.115726>.
- Qiu, P., Cui, Z., Huang, D., Tu, L., Xu, M., 2024. Mechanical characterization and decay resistance of parallel strand bamboo against white-rot and brown-rot fungi. *Structures* 65, 106682. <https://doi.org/10.1016/j.istruc.2024.106682>.
- Sánchez, C., 2009. Lignocellulosic residues: biodegradation and bioconversion by fungi. *Biotechnol. Adv.* 27, 185–194. <https://doi.org/10.1016/j.biotechadv.2008.11.001>.
- Santana, T.T., Linde, G.A., Colauto, N.B., do Valle, J.S., 2018. Metallic-aromatic compounds synergistically induce *Lentinus crinitus* laccase production. *Biocatal. Agric. Biotechnol.* 16, 625–630. <https://doi.org/10.1016/j.bcab.2018.10.018>.
- Shi, Z.-J., Xiao, L.-P., Deng, J., Sun, R.-C., 2013. Isolation and structural characterization of lignin polymer from *Dendrocalamus sinicus*. *Bioenerg. Res.* 6, 1212–1222. <https://doi.org/10.1007/s12155-013-9321-8>.
- Sohail, M., Barzkar, N., Michaud, P., Tamadoni Jahromi, S., Babich, O., Sukhikh, S., Das, R., Nahavandi, R., 2022. Cellulolytic and xylanolytic enzymes from yeasts: properties and industrial applications. *Molecules* 27, 3783. <https://doi.org/10.3390/molecules27123783>.
- Wang, F., Yu, X., Yu, Z., Cui, Y., Xu, L., Huo, S., Ding, Z., Zhao, L., Du, L., Qiu, Y., 2023. Improved laccase production by *Trametes versicolor* using Copper-Glycyl-L-Histidyl-L-Lysine as a novel and high-efficient inducer. *Front. Bioeng. Biotechnol.* 11. <https://doi.org/10.3389/fbioe.2023.1176352>.
- Wang, J., Wang, X., Zhan, T., Zhang, Y., Lv, C., He, Q., Fang, L., Lu, X., 2018. Preparation of hydro-thermal surface-densified plywood inspired by the stiffness difference in “sandwich structure” of wood. *Constr. Build. Mater.* 177, 83–90. <https://doi.org/10.1016/j.conbuildmat.2018.05.135>.

- Wang, J., Wu, X., Wang, Y., Zhao, W., Zhao, Y., Zhou, M., Wu, Y., Ji, G., 2022. Green, sustainable architectural bamboo with high light transmission and excellent electromagnetic shielding as a candidate for energy-saving buildings. *NanoMicro Lett.* 15, 11. <https://doi.org/10.1007/s40820-022-00982-7>.
- Wang, Y., Yu, Y., Zhao, F., Feng, Y., Feng, W., 2023. Multi-functional and multi-responsive layered double hydroxide-reinforced polyacrylic acid composite hydrogels as ionic skin sensors. *Adv. Compos. Hybrid. Mater.* 6, 65. <https://doi.org/10.1007/s42114-023-00653-0>.
- Wang, Y.-Y., Li, Y.-Q., Xue, S.-S., Zhu, W.-B., Wang, X.-Q., Huang, P., Fu, S.-Y., 2022. Superstrong, lightweight, and exceptional environmentally stable SiO₂@GO/bamboo composites. *ACS Appl. Mater. Interfaces* 14, 7311–7320. <https://doi.org/10.1021/acsami.1c22503>.
- Wen, J.-L., Xue, B.-L., Xu, F., Sun, R.-C., Pinkert, A., 2013. Unmasking the structural features and property of lignin from bamboo. *Ind. Crops Prod.* 42, 332–343. <https://doi.org/10.1016/j.indcrop.2012.05.041>.
- Wu, Y., Deng, L., Zhu, F., Mou, Q., Li, Xiazhen, He, L., Wang, Y., Cai, Z., Yu, Z., Ji, S., Li, Xianjun, 2024. Green and sustainable bamboo based composites with high self-bonding strength. *Compos. Part B Eng.* 287, 111849. <https://doi.org/10.1016/j.compositesb.2024.111849>.
- Xu, G., Wang, L., Liu, J., Wu, J., 2013. FTIR and XPS analysis of the changes in bamboo chemical structure decayed by white-rot and brown-rot fungi. *Appl. Surf. Sci.* 280, 799–805. <https://doi.org/10.1016/j.apsusc.2013.05.065>.
- Xu, R., Chen, J., Yan, N., Xu, B., Lou, Z., Xu, L., 2025. High-value utilization of agricultural residues based on component characteristics: potentiality and challenges. *J. Bioresour. Bioprod.* 10, 271–294. <https://doi.org/10.1016/j.jobab.2025.01.002>.
- Yang, G., Gong, Z., Luo, X., Chen, L., Shuai, L., 2023. Bonding wood with uncondensed lignins as adhesives. *Nature* 621, 511–515. <https://doi.org/10.1038/s41586-023-06507-5>.
- Yang, X., Zhao, Y., Li, W., Li, R., Wu, Y., 2019. Unveiling the pyrolysis mechanisms of hemicellulose: experimental and theoretical studies. *Energy Fuels* 33, 4352–4360. <https://doi.org/10.1021/acs.energyfuels.9b00482>.
- Yelle, D.J., Ralph, J., 2016. Phenol-formaldehyde reactivity with lignin in the wood cell wall. *Proceedings of the International Conference on Polyphenols*, July 11–15, 2016, Vienna, Austria. Ed.: Krebs, Heinz A. Publisher: Book-of-Abstracts.com. pp. 170–171. 170–171.
- Yu, Y., Zhu, R., Wu, B., Hu, Y., Yu, W., 2015. Fabrication, material properties, and application of bamboo scrimber. *Wood Sci. Technol.* 49, 83–98. <https://doi.org/10.1007/s00226-014-0683-7>.
- Zhang, Y., Wang, R., Liu, L., Wang, E., Yang, J., Yuan, H., 2023. Distinct lignocellulolytic enzymes produced by *Trichoderma harzianum* in response to different pretreated substrates. *Bioresour. Technol.* 378, 128990. <https://doi.org/10.1016/j.biortech.2023.128990>.
- Zhao, L., Li, W., Cheng, Y., Zhao, J., Tian, D., Huang, M., Shen, F., 2024. Preparation and evaluation of lignin-phenol-formaldehyde resin as wood adhesive using unmodified lignin. *Ind. Crops Prod.* 211, 118168. <https://doi.org/10.1016/j.indcrop.2024.118168>.
- Zhao, S., Abu-Omar, M.M., 2016. Renewable epoxy networks derived from lignin-based monomers: effect of cross-linking density. *ACS Sustain. Chem. Eng.* 4, 6082–6089. <https://doi.org/10.1021/acssuschemeng.6b01446>.
- Zheng, Y., Zhou, C., Zhang, P., Wang, Y., 2023. Comparison of mechanical performance uncertainties for sustainable high-performance bamboo/wood composites. *Constr. Build. Mater.* 403, 132740. <https://doi.org/10.1016/j.conbuildmat.2023.132740>.
- Zhou, Q., Zhao, Z., Wang, L., Wang, J., Fu, L., Cui, J., Liu, G., Yang, J., Fu, Y., 2025. Immobilized enzyme microreactor system with bamboo-based cellulose nanofibers for efficient biotransformation of phytochemicals. *J. Bioresour. Bioprod.* 10, 224–238. <https://doi.org/10.1016/j.jobab.2025.03.004>.
- Zou, M., Tang, Q., Guo, W., 2022. High-strength wood-based composites via laminated delignified wood veneers with different adhesive contents for structural applications. *Polym. Compos.* 43, 2746–2758. <https://doi.org/10.1002/pc.26571>.